Mechanochromic luminescence properties of fluoro-substituted pinene-containing cyclometalated platinum(II) complexes with multiple triplet excited states

Qian-Ying Yang [a], Hua-Hong Zhang [a], Xiao-Wei Qi [a], Shi-Shu Sun [a], Da-Shuai Zhang [a], Li-Zhi Han [a], Xiao-Peng Zhang [a,*], Zai-Feng Shi [a]

[a] College of Chemistry and Chemical Engineering, Key Laboratory of Water Pollution Treatment & Resource Reuse of Hainan Province, Hainan Normal University, Haikou 571158, P.R. China

Corresponding author: X.-P. Zhang

Email: zxp_inorganic@126.com

Materials and methods, synthesis, crystal structures, solution spectroscopic properties, TD-DFT calculation results, mechanochromic luminescence and references

Table of Contents

1. NMR spectra

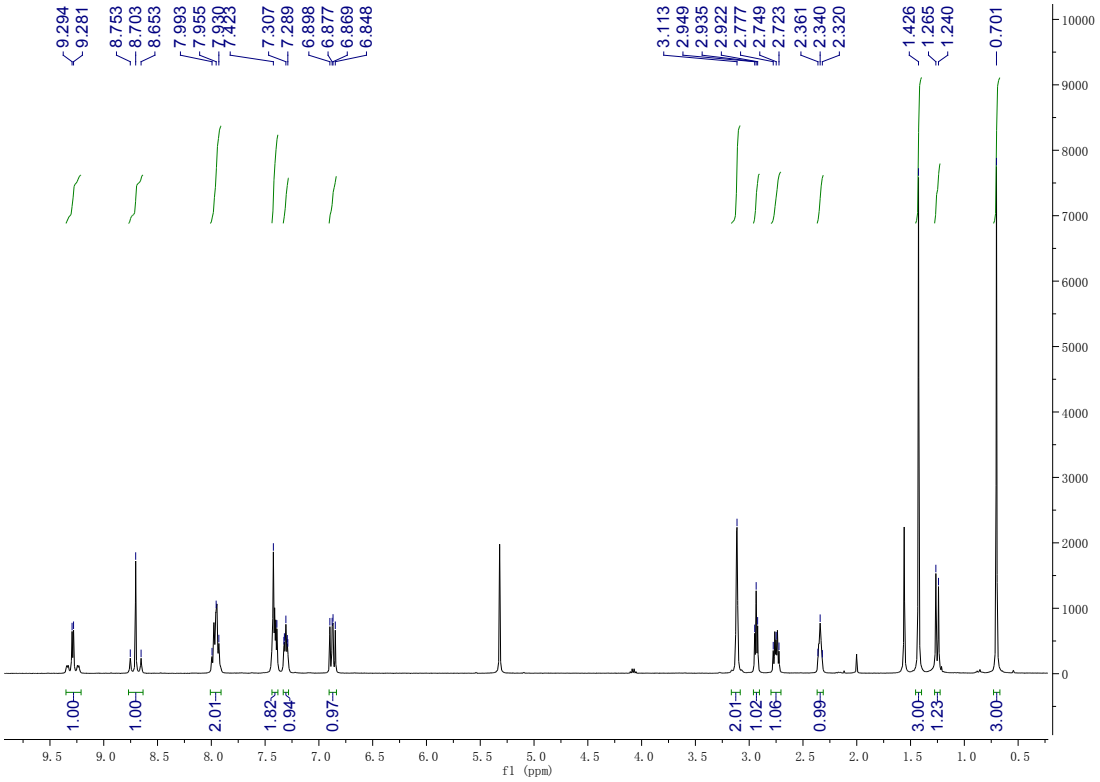

Fig. S1 ^{1}H NMR of **(−)-2**

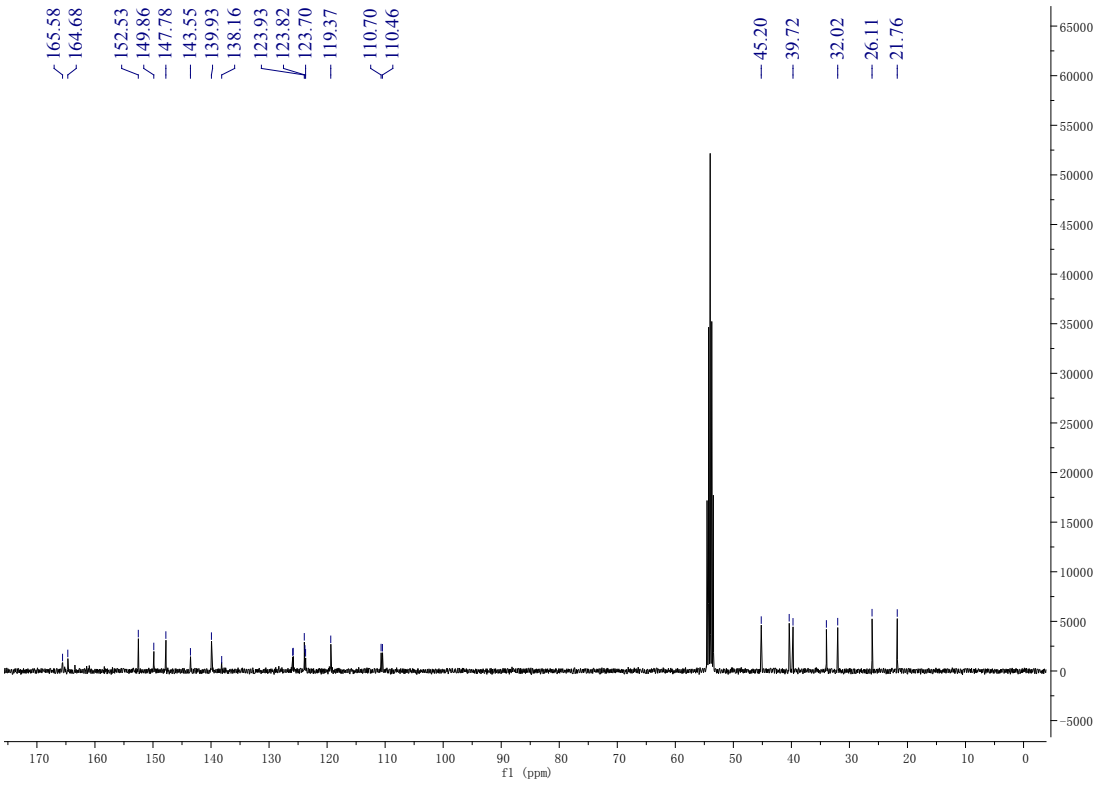

Fig. S2 ^{13}C NMR of **(−)-2**

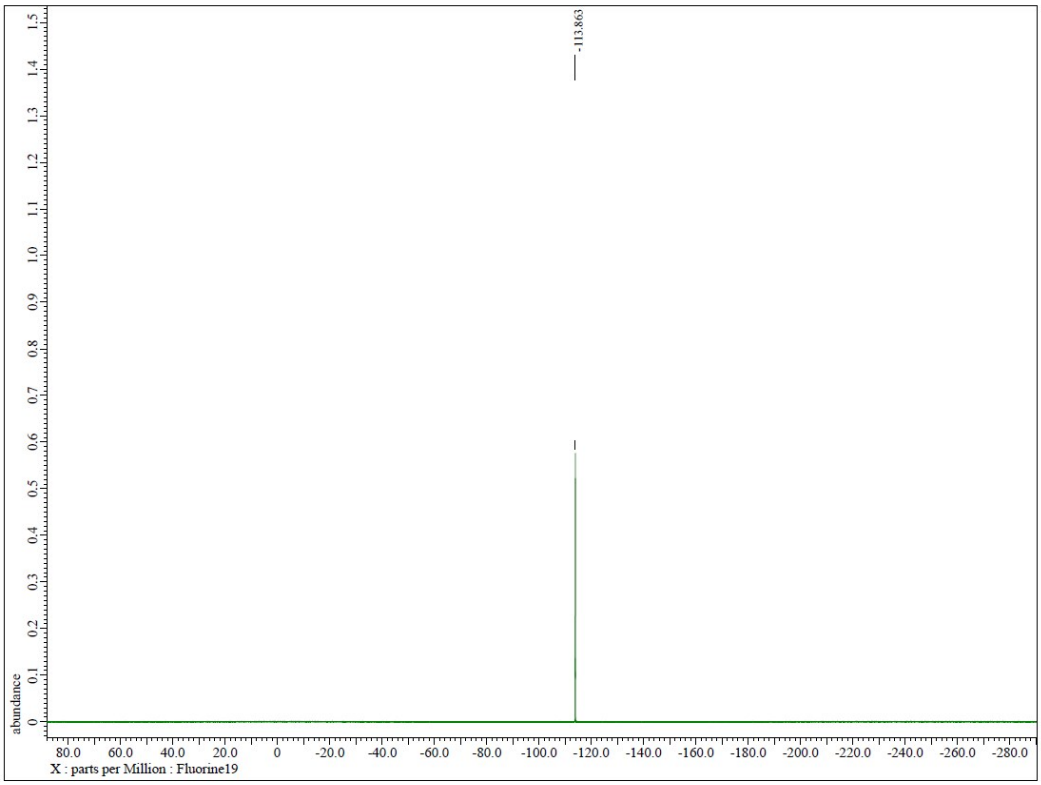

Fig. S3 ^{19}F NMR of **(−)-2**

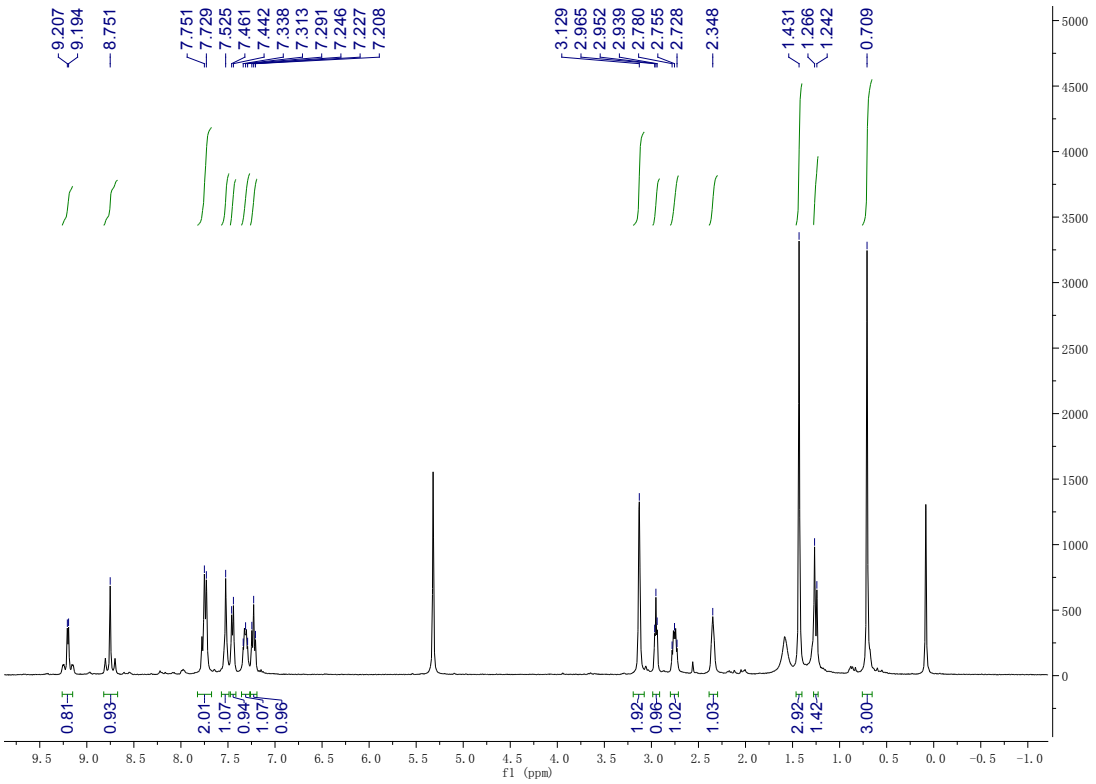

Fig. S4 ^{1}H NMR of **(−)-3**

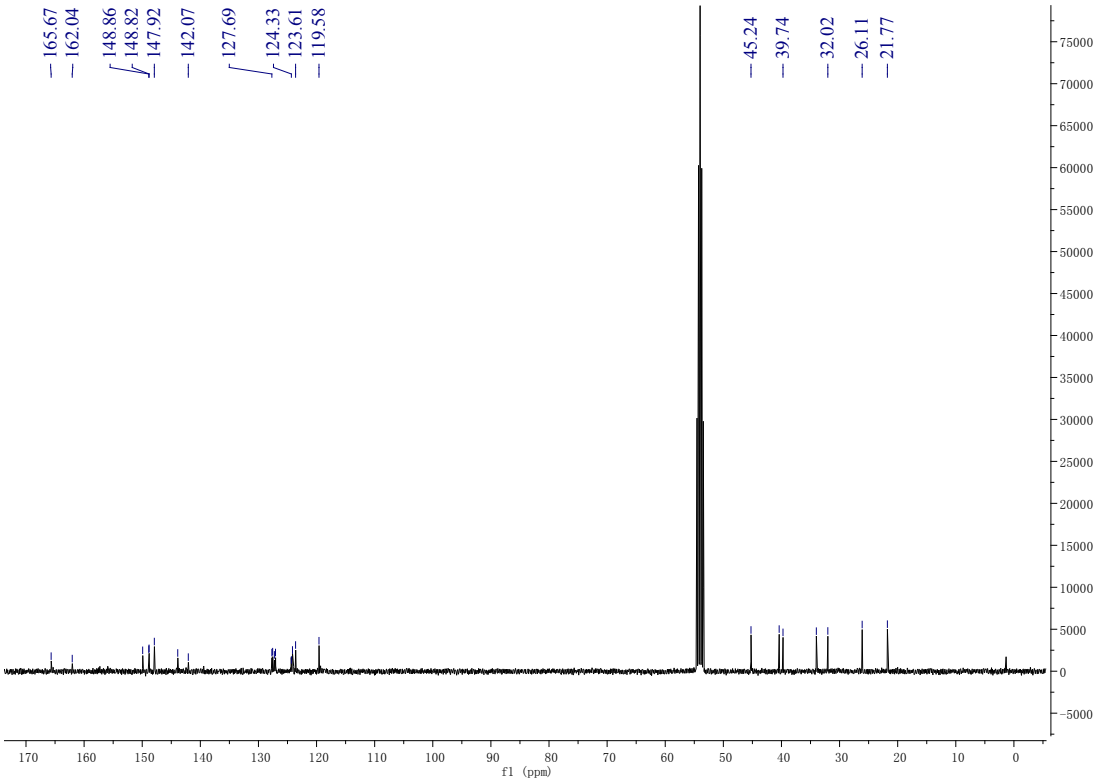

Fig. S5 ^{13}C NMR of **(−)-3**

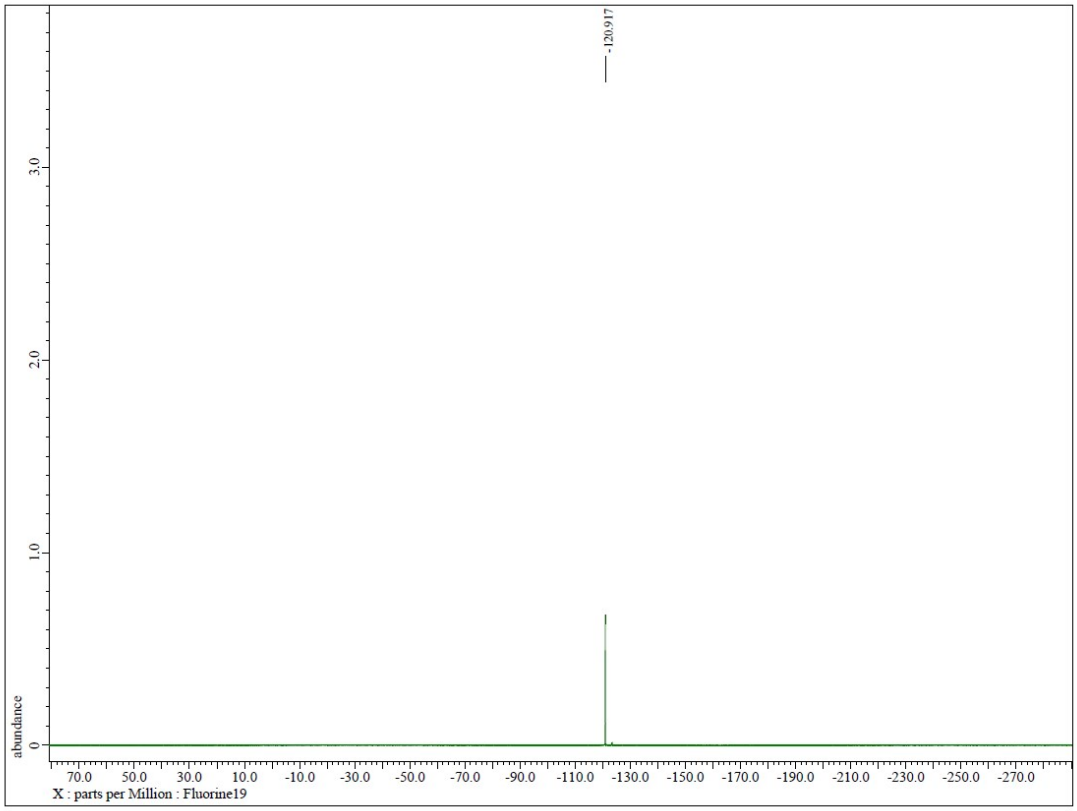

Fig. S6 ^{19}F NMR of **(−)-3**

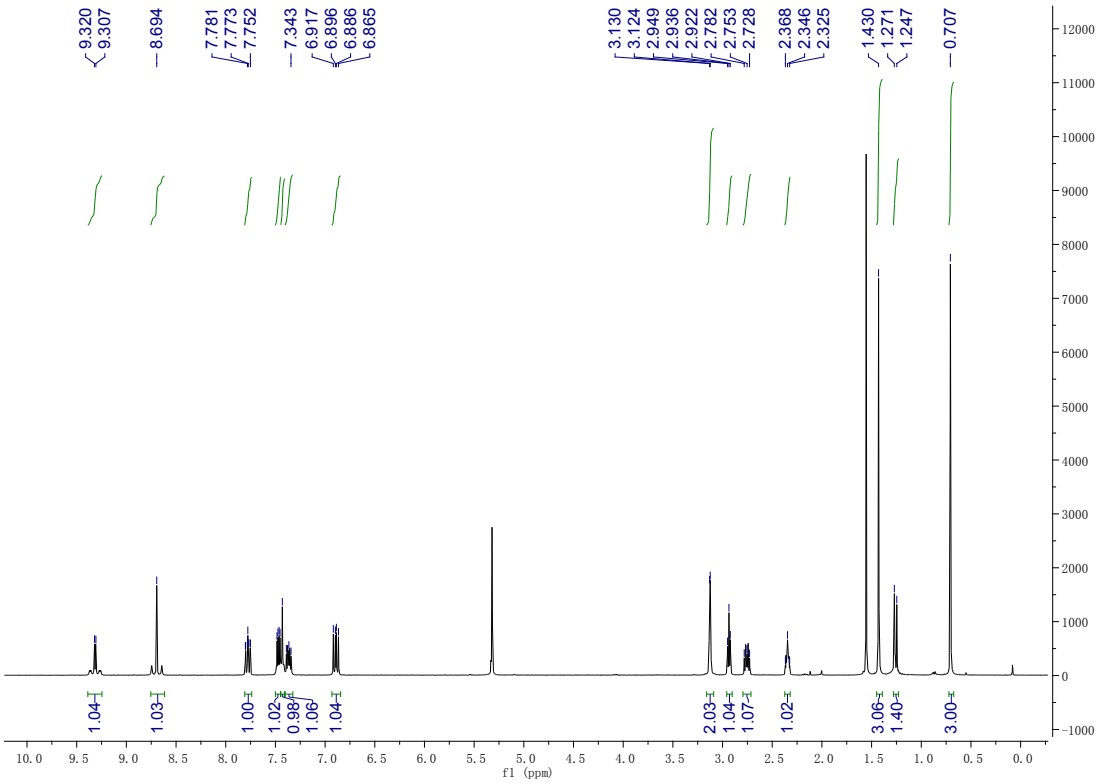

Fig. S7 ^{1}H NMR of **(−)-4**

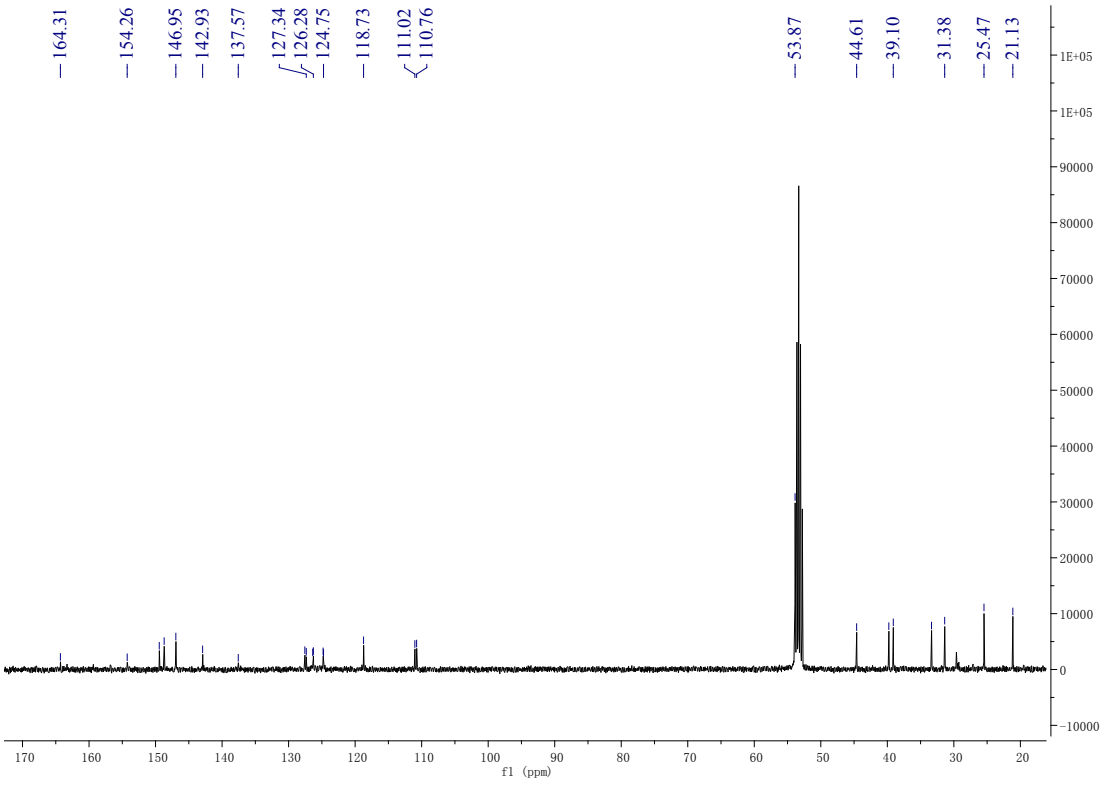

Fig. S8 ^{13}C NMR of **(−)-4**

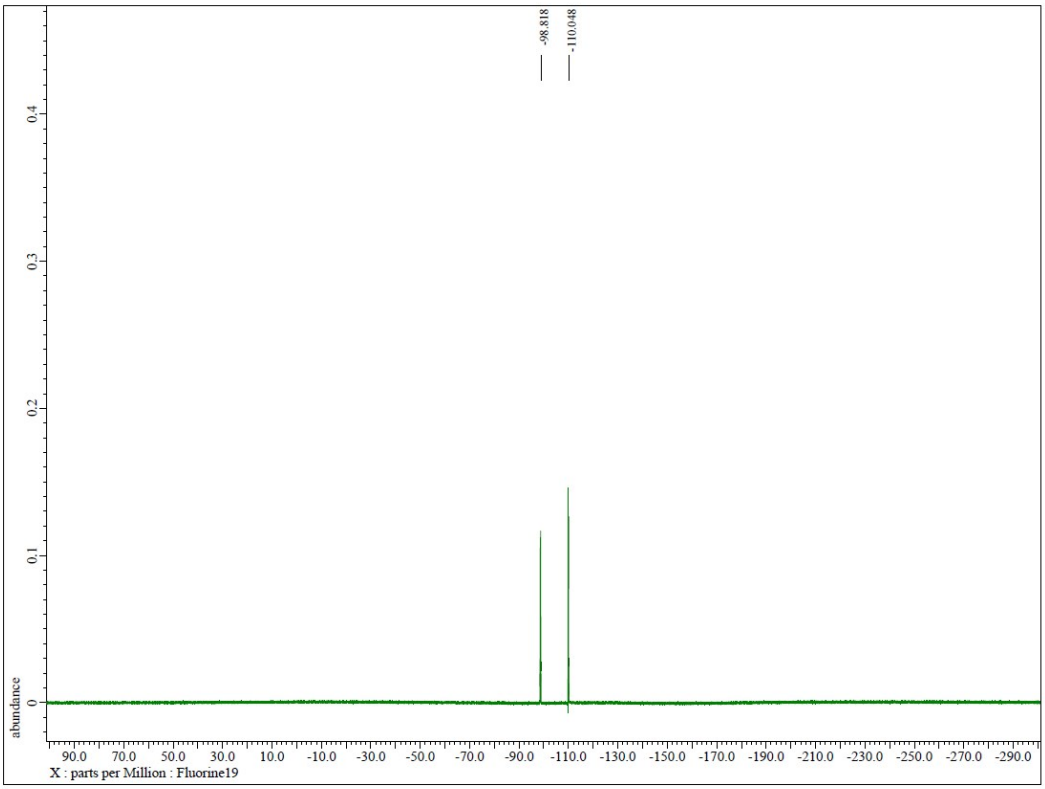

Fig. S9 ^{19}F NMR of **(−)-4**

2. Crystallographic data

Table S1 Crystallographic data of crystal forms **(−)-2-Y-1**, **(−)-2-Y-2**, **(+)-2-O-1**, **(−)-3-Y** and (−)-**4-O**

	(−)-**2-Y-1**	(−)-**2-Y-2**	(+)-**2-O-1**	(−)-**3-Y**	(−)-**4-O**
Formula	$C_{23}H_{20}ClFN_2Pt_2$	$C_{23.94}H_{20.94}Cl_{3.81}FN_2Pt$	$C_{23}H_{20}ClFN_2Pt$	$C_{24}H_{22}Cl_3FN_2Pt$	$C_{23}H_{19}ClF_2N_2Pt$
Mr/g mol^{-1}	573.95	685.86	573.95	658.87	591.94
crystal system	Orthorhombic	Triclinic	Monoclinic	Triclinic	Monoclinic
Space group	$P2_12_12_1$	$P1$	$P2_1$	$P1$	$P2_1$
a/Å	10.0122(3)	9.3078(6)	7.1917(7)	7.1424(5)	7.1804(3)
b/Å	13.8750(4)	13.9840(10)	18.1841(17)	9.1357(9)	18.1579(8)
c/Å	27.4999(10)	20.3736(16)	14.8761(14)	18.4824(14)	14.8582(7)
α/ °	90.00	74.719(6)	90.00	96.097(8)	90.00
β/ °	90.00	77.334(6)	99.525(5)	100.086(6)	97.719(2)
γ/ °	90.00	89.414(6)	90.00	92.237(7)	90.00
V/Å^3	3820.3(2)	2492.6(3)	1918.6(3)	1178.59(17)	1919.67(15)
Z	8	4	4	2	4
T /K	153(2)	153(2)	193(2)	298(2)	213(2)
Radiation, λ /Å	0.71073	0.71073	1.34139	0.71073	0.71073
D_{calcd}, g/cm^{-3}	1.996	1.828	1.987	1.857	2.048
μ/mm^{-1}	7.506	6.060	10.368	6.315	7.480
F(000)	2208	1322	1104	636	1136
θ range/°	2.085 to 27.102	2.692 to 29.762	3.367 to 57.299	2.394 to 25.027	1.781 to 25.351
Reflections	34734	22310	9945	8105	27737
Unique	8386	15837	3962	5762	7010
R_{int}	0.0533	0.0736	0.0655	0.0632	0.0539
Reflections with $F^2 > 2\sigma(F^2)$	7721	8614	3454	4761	6381
Number of parameters	509	1129	510	492	528
Goodness-of-fit on F^2	1.033	1.029	1.078	1.055	0.890
R_1 [$F^2 > 2\sigma(F^2)$]	0.0288	0.0657	0.0697	0.0792	0.0297
wR_2 (all data)	0.0517	0.1528	0.1927	0.2332	0.0702
$\Delta\rho_{max}$, $\Delta\rho_{min}$/eÅ^{-3}	0.954, -1.002	2.461, -1.647	2.508, -1.595	2.259, -1.637	1.207, -0.762
Flack parameter	-0.016(5)	0.07(2)	0.11(4)	0.04(2)	0.185(10)
CCDC number	2066698	2066700	2066699	2066697	2066696.

Table S2 Bond lengths of complexes **(−)-2-Y-1**, **(−)-2-Y-2**, **(+)-2-O-1**, **(−)-3-Y** and (−)-**4-O** determined by X-ray single crystal diffraction.

Bond Lengths	(−)-**2**-Y-1	(−)-**2**-Y-2	(+)-**2**-O-1	(−)-**3-Y**	(−)-**4-O**

Pt1−C1	1.907(5)	1.95(4)	2.01(4)	1.873(9)	1.866(9)
Pt1−N1	2.035(4)	2.05(3)	2.05(3)	2.061(10)	2.024(7)
Pt1−N2	2.021(4)	2.03(3)	2.01(3)	2.109(10)	2.017(7)
Pt1−Cl1	2.4183(12)	2.440(11)	2.408(8)	2.420(11)	2.422(2)
Pt2−C2	1.911(5)	1.89(3)	1.83(4)	1.910(11)	1.921(10)
Pt2−N3	2.026(4)	1.98(3)	2.00(3)	2.075(10)	1.999(7)
Pt2−N4	2.026(4)	1.98(3)	2.06(3)	1.956(16)	2.029(8)
Pt2−Cl2	2.4239(13)	2.387(10)	2.435(9)	2.427(13)	2.416(2)
Pt3−C3		1.859(15)			
Pt3−N5		1.94(3)			
Pt3−N6		2.02(2)			
Pt3−Cl3		2.405(10)			
Pt4−C4		2.01(3)			
Pt4−N7		2.10(3)			
Pt4−N8		2.043(13)			
Pt4−Cl4		2.437(10)			

Table S3 Bond angles around Pt(II) nucleus of complexes **(−)-2-Y-1**, **(−)-2-Y-2**, **(+)-2-O-1**, **(−)-3-Y** and (−)-**4-O**.

Bond Angles	**(−)-2-Y-1**	**(−)-2-Y-2**	**(+)-2-O-1**	**(−)-3-Y**	**(−)-4-O**
C1−Pt1−N1	80.8(2)	86.6(13)	82.2(13)	86.8(4)	82.4(3)
C1−Pt1−N2	80.05(19)	79.4(13)	78.2(14)	74.1(3)	80.6(3)
C1−Pt1−Cl1	177.99(16)	174.0(9)	176.3(10)	172.0(5)	175.5(2)
N1−Pt1−N2	160.80(17)	166.0(11)	160.3(11)	160.7(5)	163.0(3)
N1−Pt1−Cl1	99.15(13)	96.6(8)	98.9(8)	96.1(4)	98.9(2)
N2−Pt1−Cl1	100.04(13)	97.4(9)	100.8(9)	103.2(4)	98.0(2)
C2−Pt2−N3	81.3(2)	79.9(13)	79.5(12)	76.0(4)	81.3(3)
C2−Pt2−N4	80.05(19)	80.7(14)	82.2(13)	85.7(6)	81.1(3)
C2−Pt2−Cl2	177.85(15)	178.4(10)	179.1(10)	178.2(5)	178.5(2)
N3−Pt2−N4	161.25(18)	160.5(11)	161.5(11)	161.6(7)	162.3(3)
N3−Pt2−Cl2	99.00(13)	100.0(9)	100.7(8)	103.1(5)	99.0(2)
N4−Pt2−Cl2	99.71(13)	99.5(8)	97.6(9)	95.3(7)	98.5(2)
C3−Pt3−N5		79.2(11)			
C3−Pt3−N6		80.0(11)			
C3−Pt3−Cl3		178.3(8)			
N5−Pt3−N6		159.2(11)			
N5−Pt3−Cl3		102.4(8)			
N6−Pt3−Cl3		98.5(8)			
C4−Pt4−N7		81.7(11)			
C4−Pt4−N8		82.2(10)			
C4−Pt4−Cl4		176.1(9)			

N7−Pt4−N8	163.7(8)
N7−Pt4−Cl4	98.1(7)
N8−Pt4−Cl4	98.1(6)

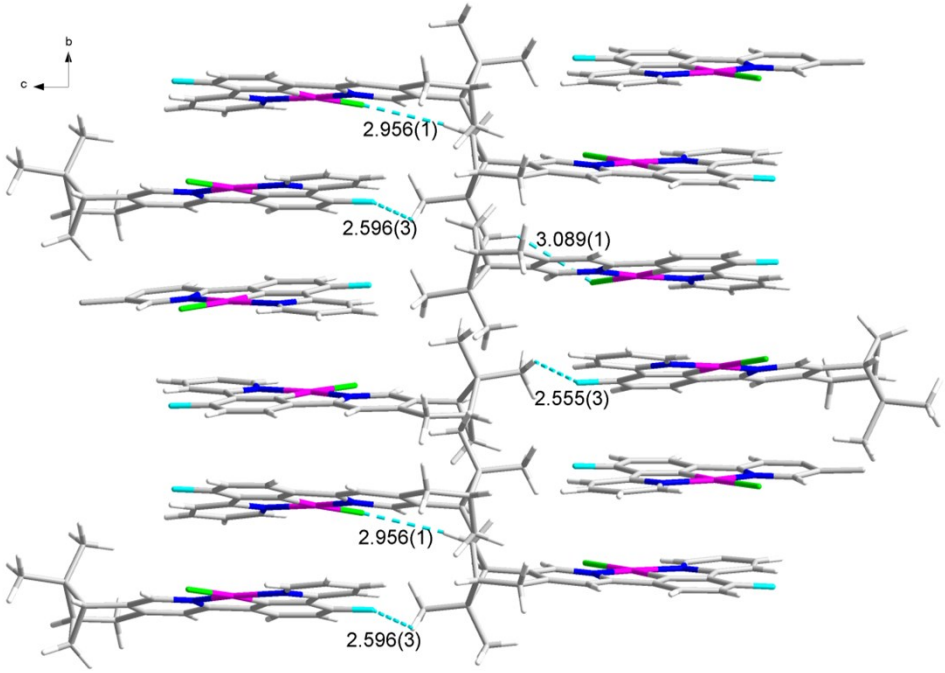

Fig. S10 The packing structure between the neighbouring columns of forms **(−)-2-Y-1** with cyan dashed lines indicating C−H···X (F or Cl) contacts. The unit of bond length is Å.

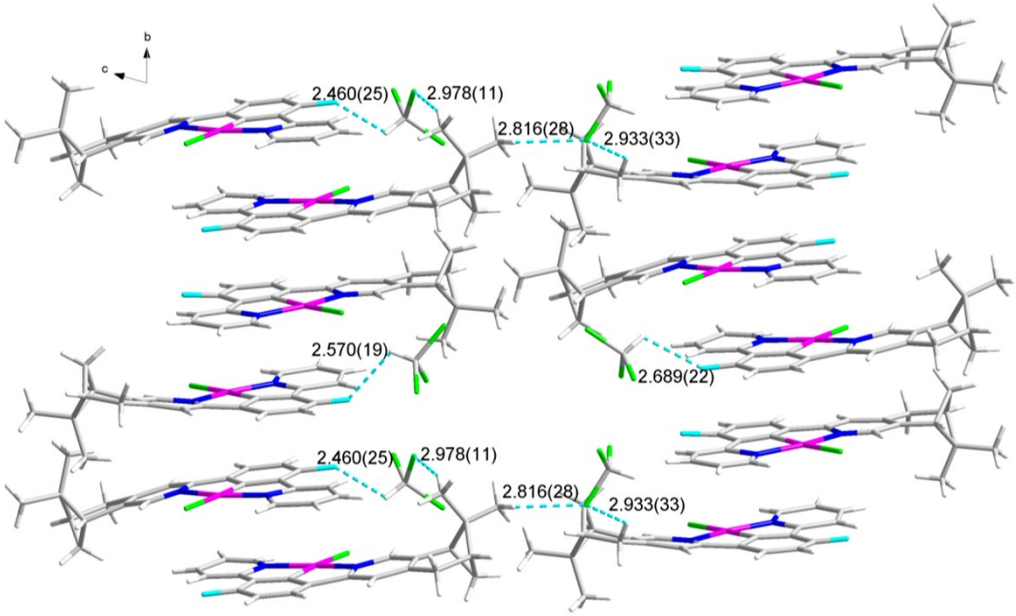

Fig. S11 The packing structure between the neighbouring columns of forms **(−)-2-Y-2** with cyan dashed lines indicating C−H···X (F or Cl) contacts. The unit of bond length is Å.

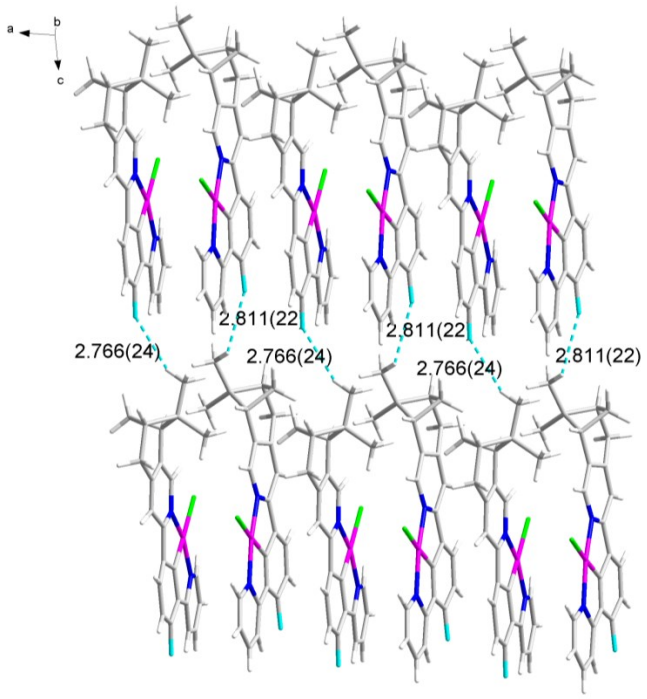

Fig. S12 The packing structure between the neighbouring columns of forms **(+)-2-O-1** with cyan dashed lines indicating C−H···X (F or Cl) contacts. The unit of bond length is Å.

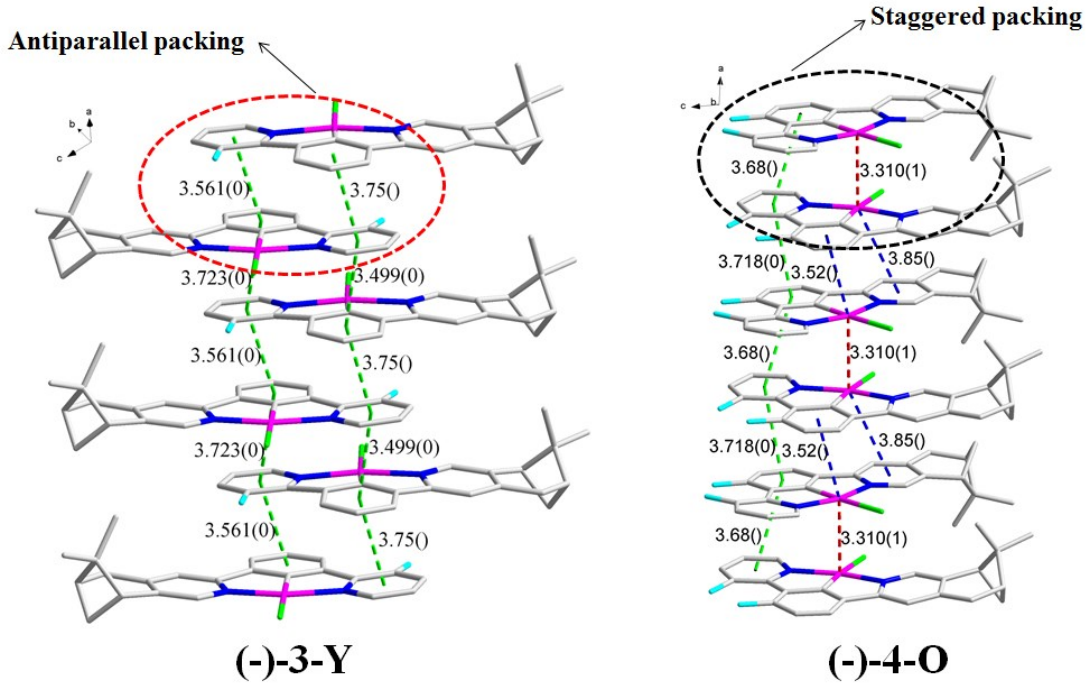

(-)-3-Y **(-)-4-O**

Fig. S13 Crystal packing structures of (−)-**3-Y** and (−)-**4-O** with red dashed lines indicating the Pt···Pt distances, green dashed lines indicating the π–π distances and blue dashed lines indicating the Pt–π distances. H atoms and solvent molecules are omitted for clarity. The unit of bond length is Å.

3. Solution spectroscopic properties

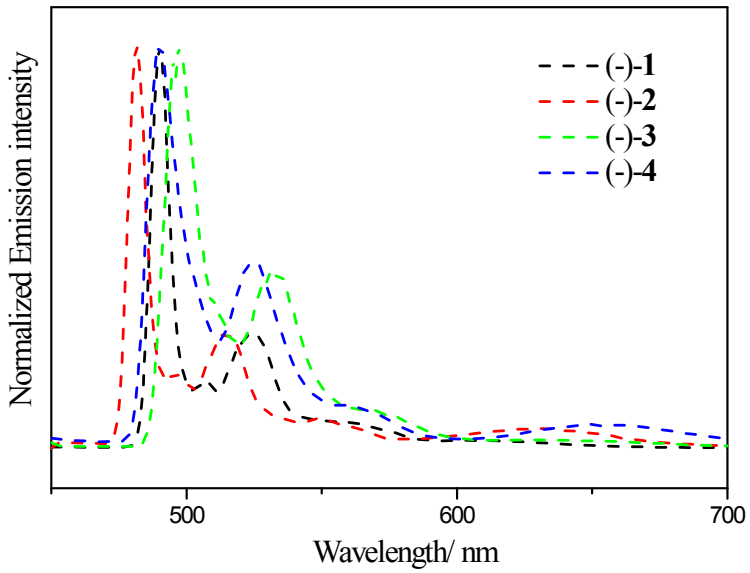

Fig. S14 Emission spectra (λ_{ex} = 420 nm) of Pt(NCN)Cl complexes in CH_2Cl_2 (5×10^{-5} mol·L^{-1}) at 77 K.

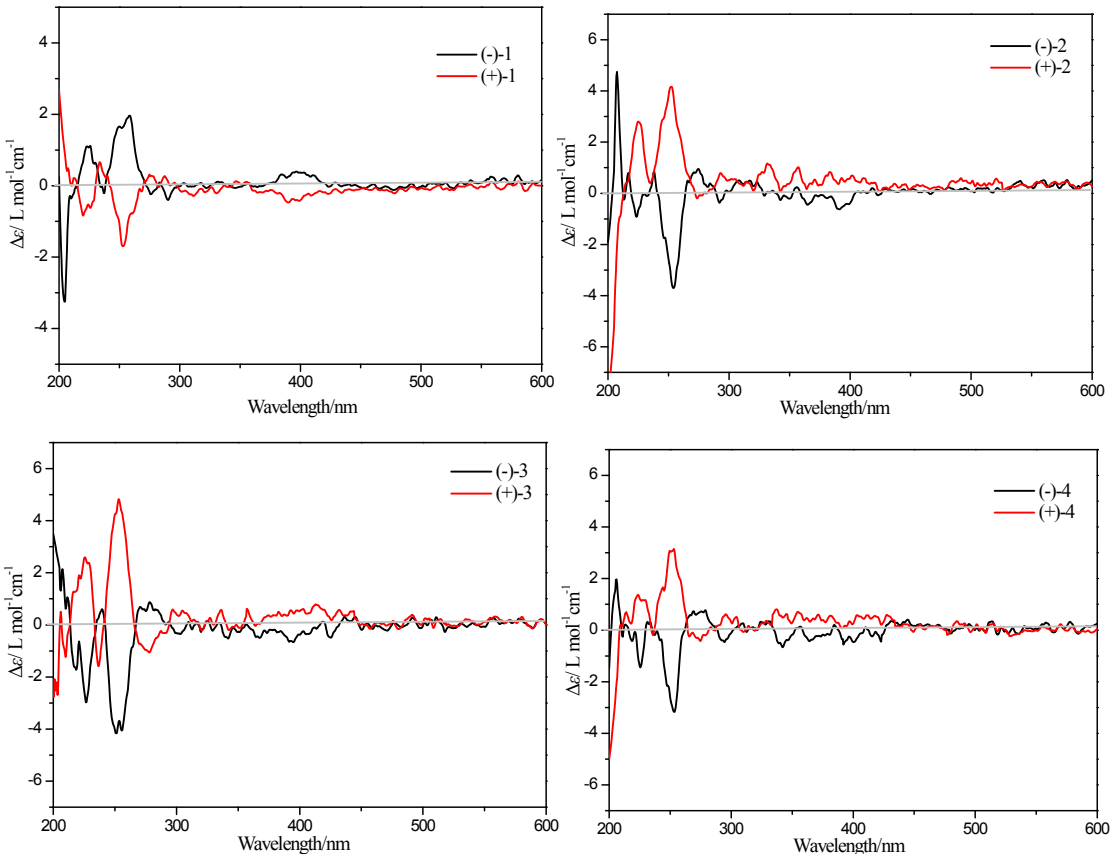

Fig. S15 ECD spectra of Pt(NCN)Cl complexes in CH_2Cl_2 (5×10^{-5} mol·L^{-1}).

4. TD-DFT calculation results

Table S4 TDDFT-calculated electronic transitions, oscillator strength (*f*), description and characters for (−)-**1** to (−)-**4**.

complex	excited state	ΔE (nm)	*f*	description	percentage	character
(−)-**1**	S_1	337.87	0.1100	HOMO→LUMO	84.2%	LC/MLCT/ILCT/LLCT
				HOMO-1→LUMO	6.1%	LC/MLCT/ILCT
	T1	667.01	0.0000	HOMO→LUMO	73.1%	LC/MLCT/ILCT/LLCT
				HOMO-1→LUMO	16.0%	LC/MLCT/ILCT
(−)-**2**	S_1	334.05	0.0467	HOMO→LUMO	79.4%	LC/MLCT/ILCT/LLCT
				HOMO-1→LUMO	8.8%	LC/MLCT/ILCT
	T1	607.70	0.0000	HOMO→LUMO	56.8%	LC/MLCT/ILCT/LLCT
				HOMO-1→LUMO	27.0%	LC/MLCT/ILCT
(−)-**3**	S_1	349.28	0.1079	HOMO→LUMO	87.1%	LC/MLCT/ILCT/LLCT
				HOMO-1→LUMO	7.0%	LC/MLCT/ILCT
	T1	667.47	0.0000	HOMO→LUMO	72.5%	LC/MLCT/ILCT/LLCT
				HOMO-1→LUMO	16.1%	LC/MLCT/ILCT
(−)-**4**	S_1	345.00	0.0719	HOMO→LUMO	81.1%	LC/MLCT/ILCT/LLCT
				HOMO-1→LUMO	11.6%	LC/MLCT/ILCT
	T1	625.91	0.0000	HOMO→LUMO	54.6%	LC/MLCT/ILCT/LLCT
				HOMO-1→LUMO	30.1%	LC/MLCT/ILCT

Table S5 DFT-calculated molecular orbital contribution of optimized ground-state structures (in %)

complex	orbital	contribution
(−)-**1**	HOMO-1	Bz (37.7%), Py (13.4%), P-Py (23.7%), Pt (20.6%), Cl (0.5%)
	HOMO	Bz (41.4%), Py (5.0%), P-Py (7.7%), Pt (33.4%), Cl (11.6%)
	LUMO	Bz (32.5%), Py (57.3%), P-Py (4.9%), Pt (4.4%), Cl (0.2%)
(−)-**2**	HOMO-1	Bz (38.8%), Py (14.5%), P-Py (20.5%), Pt (19.8%), Cl (2.3%)
	HOMO	Bz (40.9%), Py (3.0%), P-Py (11.2%), Pt (31.6%), Cl (11.7%)
	LUMO	Bz (27.9%), Py (44.0%), P-Py (5.7%), Pt (6.6%), Cl (0.4%)
(−)-**3**	HOMO-1	Bz (39.3%), Py (12.8%), P-Py (24.6%), Pt (18.2%), Cl (0.7%)
	HOMO	Bz (41.6%), Py (5.5%), P-Py (8.2%), Pt (32.5%), Cl (11.4%)
	LUMO	Bz (25.0%), Py (64.3%), P-Py (4.0%), Pt (5.8%), Cl (0.3%)
(−)-**4**	HOMO-1	Bz (40.5%), Py (15.4%), P-Py (19.8%), Pt (17.7%), Cl (3.2%)
	HOMO	Bz (42.2%), Py (3.1%), P-Py (12.3%), Pt (30.1%), Cl (11.0%)
	LUMO	Bz (24.6%), Py (63.3%), P-Py (4.6%), Pt (6.5%), Cl (0.4%)

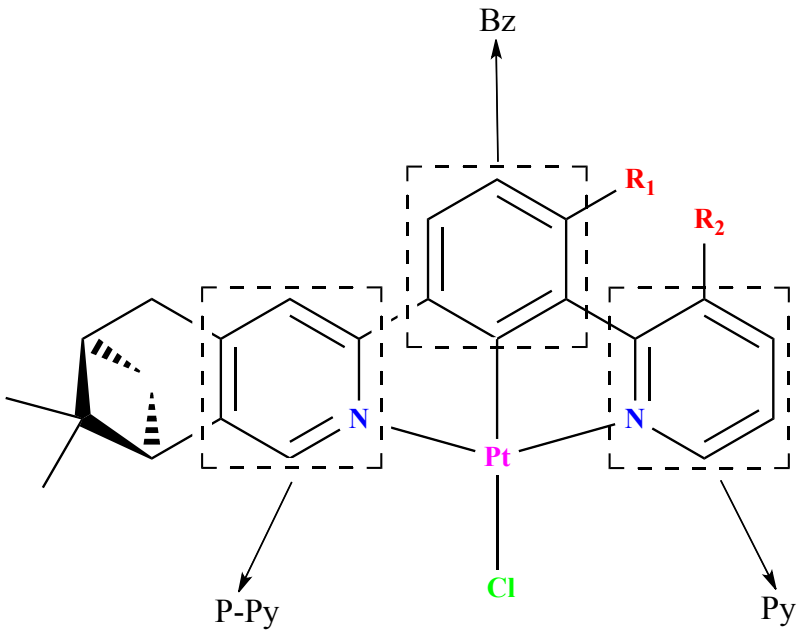

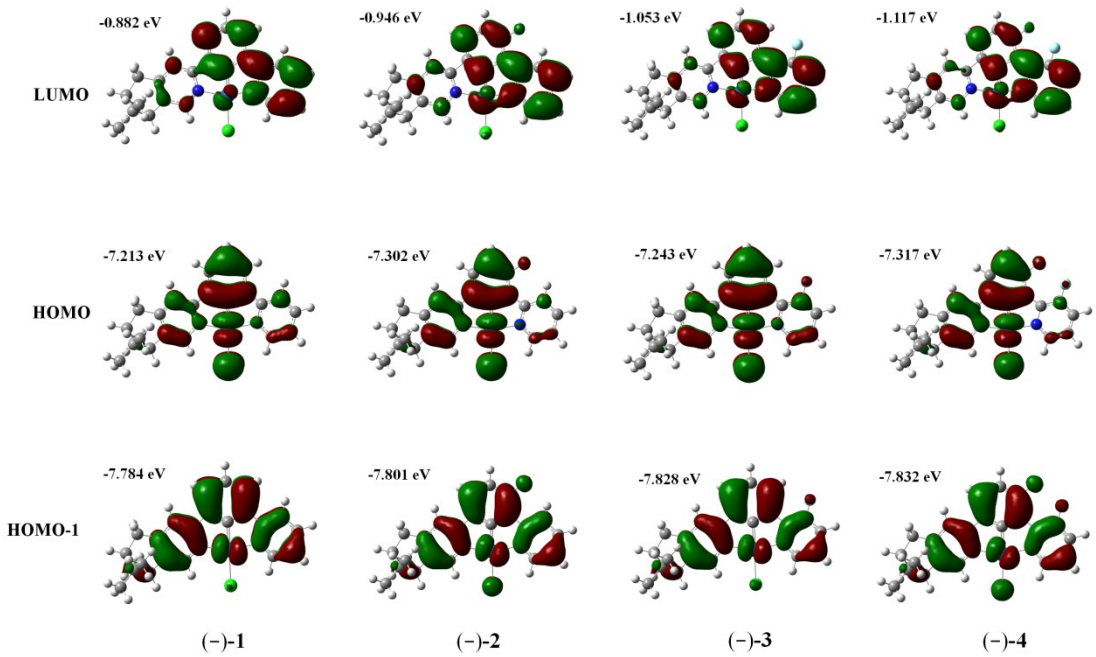

Fig. S16 Frontier molecular orbitals ofFrontier molecular orbitals of Pt(NCN)Cl complexes.

5. Mechanochromic luminescence

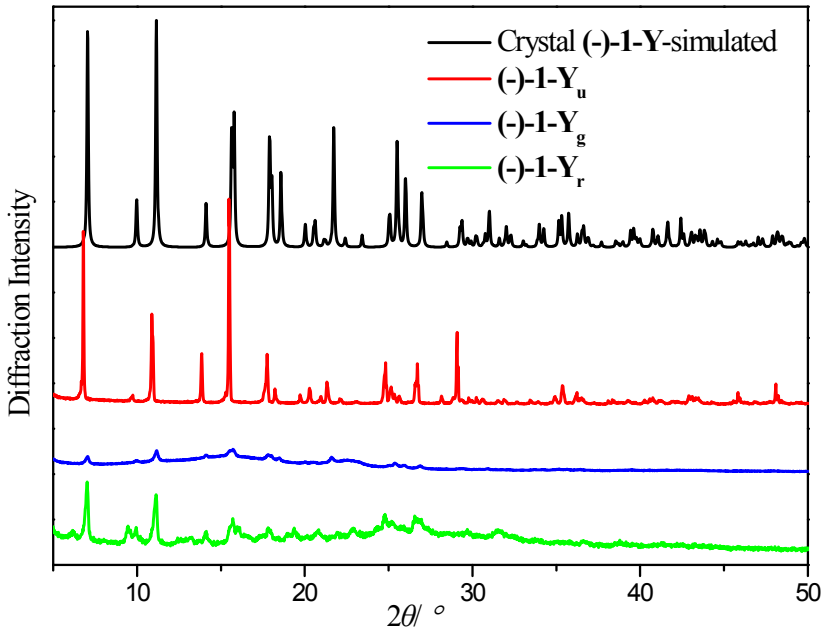

Fig. S17 XRD Patterns of (−)-**1-Y$_u$** in the reversible mechanochromic luminescence process.

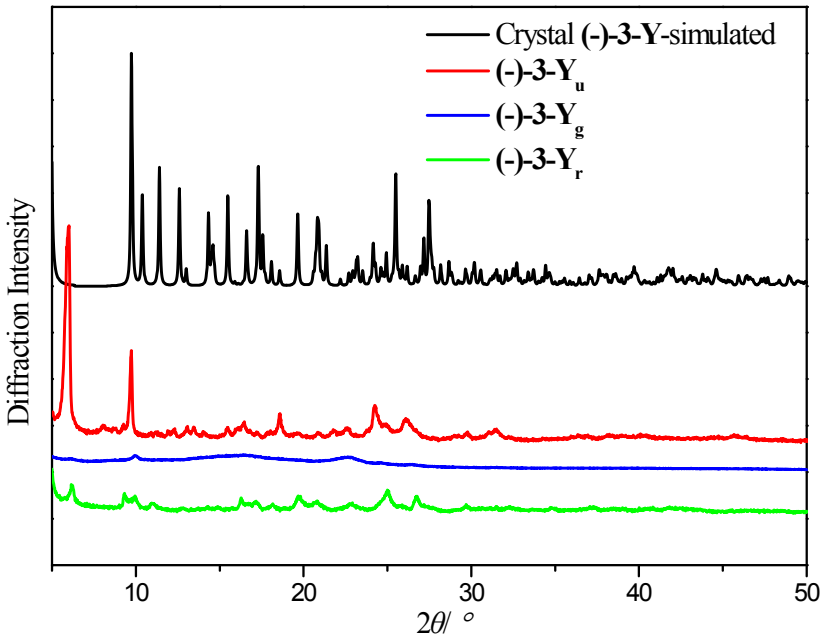

Fig. S18 XRD Patterns of (−)-**3-Y$_u$** in the reversible mechanochromic luminescence process.

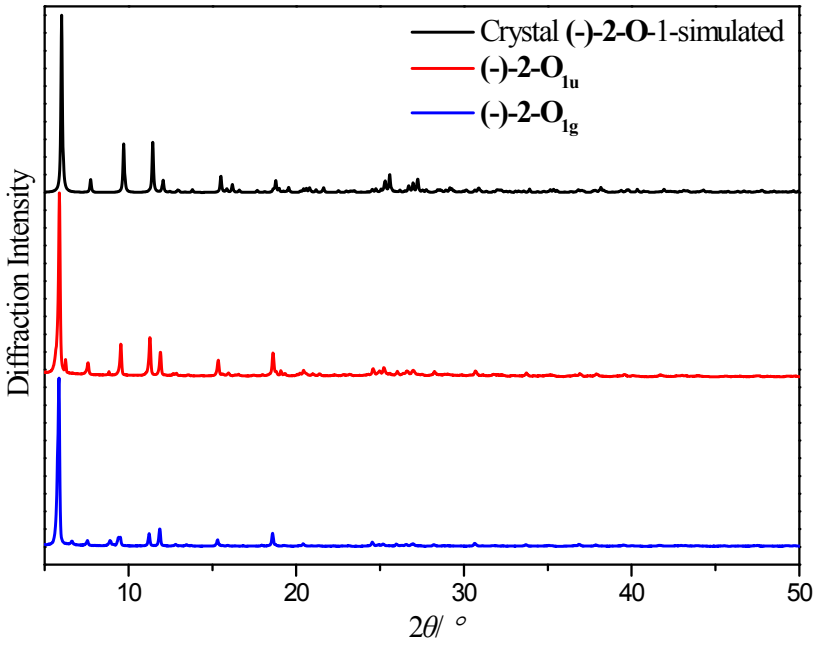

Fig. S19 XRD Patterns of (−)-**2-O$_{1u}$** in the grinding process.

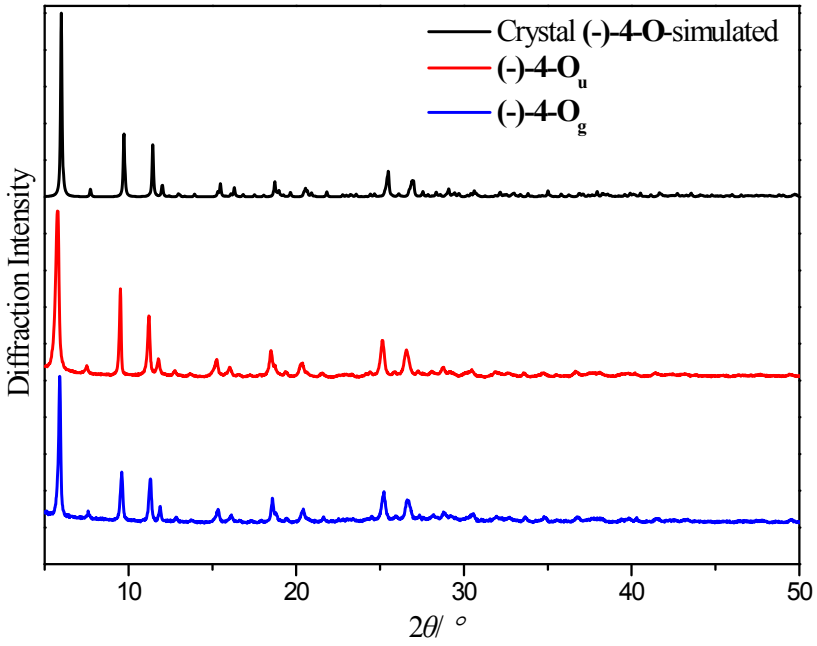

Fig. S20 XRD Patterns of (−)-**4-O$_{u}$** in the grinding process.

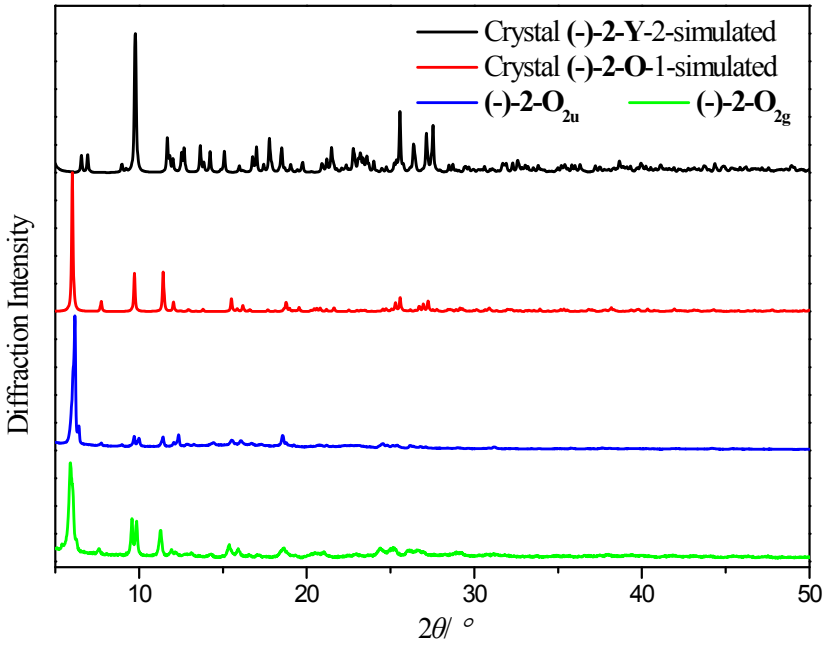

Fig. S21 XRD Patterns of (−)-**2-O$_{2u}$** in the grinding process.

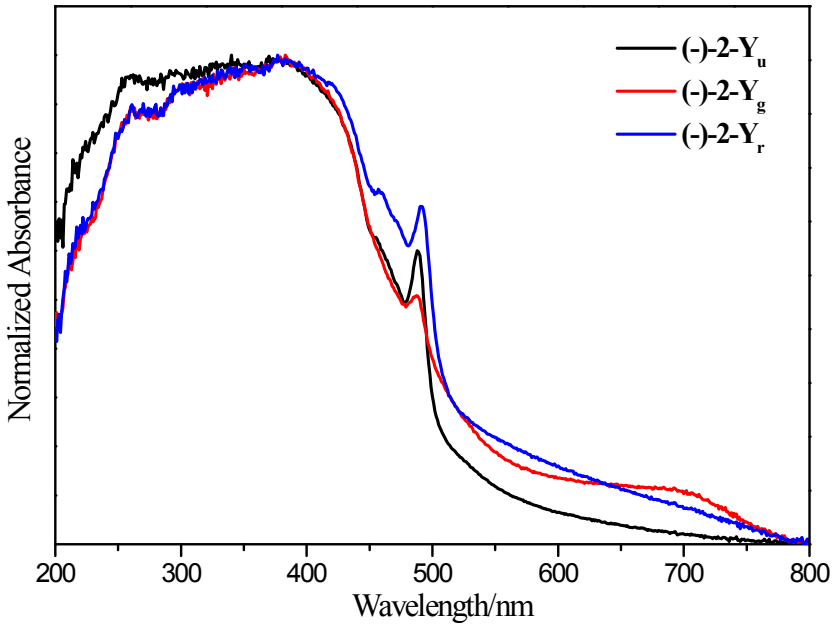

Fig. S22 Solid-state absorption spectra of (−)-**2-Y$_u$** in the mechanochromic process.

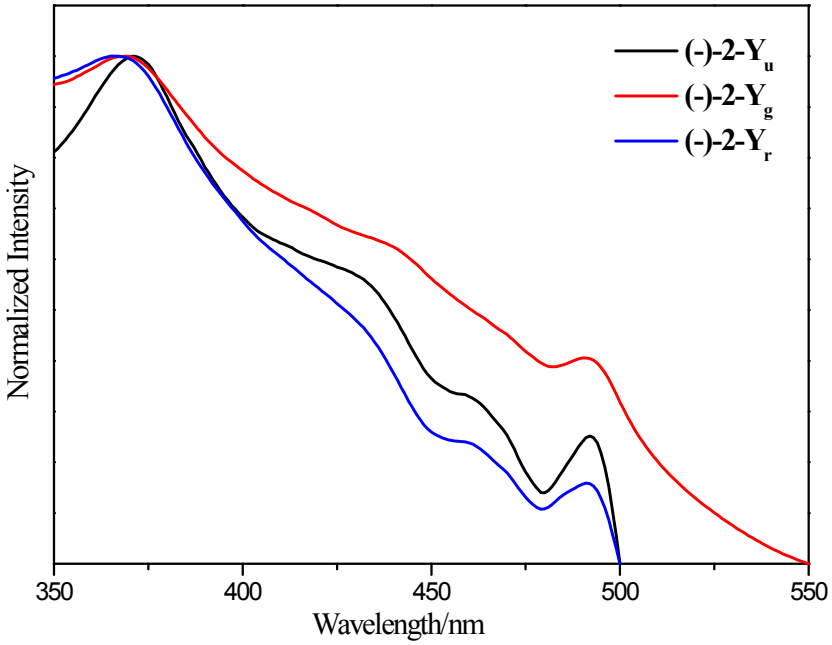

Fig. S23 Solid-state excitation spectra of (−)-**2-Y$_u$** in the mechanochromic process. The excitation spectra were monitored at the maximum emission peaks (λ_{em} = 563 nm for (−)-**2-Y$_u$** and (−)-**2-Y$_r$**; λ_{em} = 623 nm for (−)-**2-Y$_g$**).

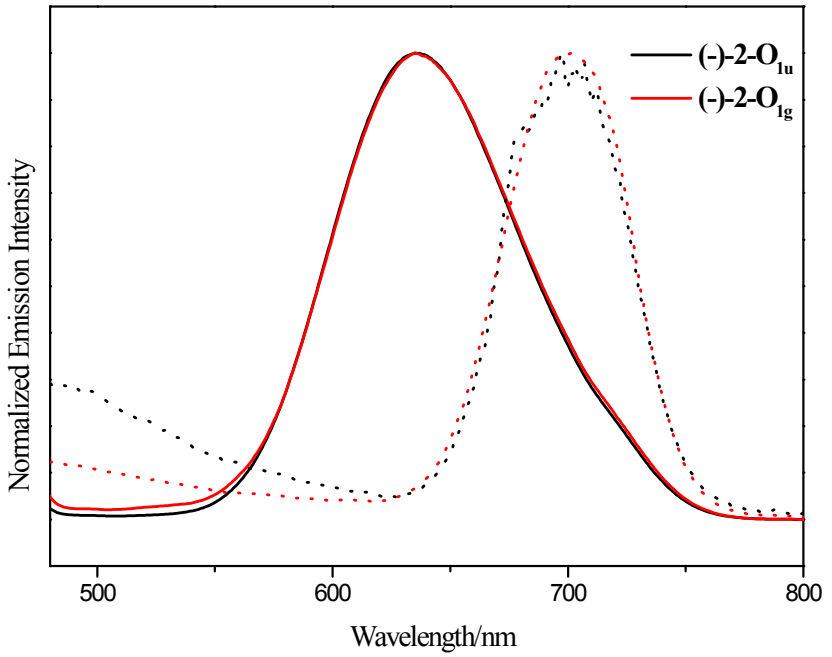

Fig. S24 Solid-state emission spectra (λ_{ex} = 420 nm) of (−)-**2-O$_{1u}$** in the grinding process at RT (solid line) and 77 K (dot line).

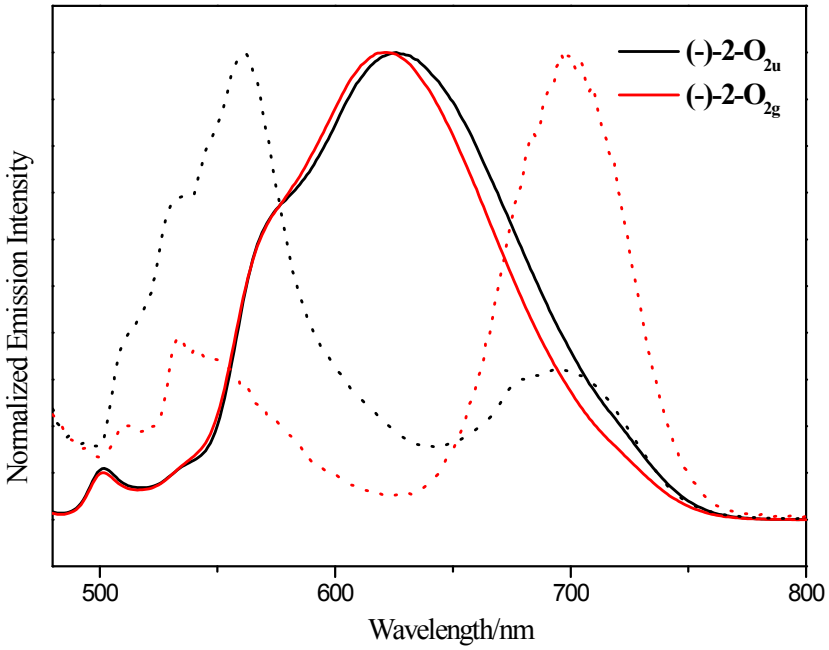

Fig. S25 Solid-state emission spectra (λ_{ex} = 420 nm) of (−)-**2-O$_{2u}$** in the grinding process at RT (solid line) and 77 K (dot line).

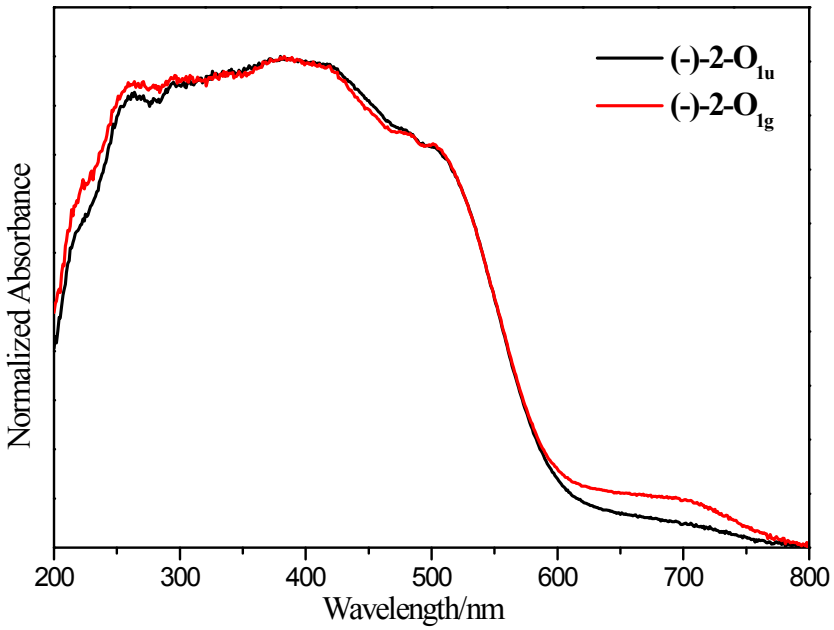

Fig. S26 Solid-state absorption spectra of (−)-**2-O$_{1u}$** in the grinding process.

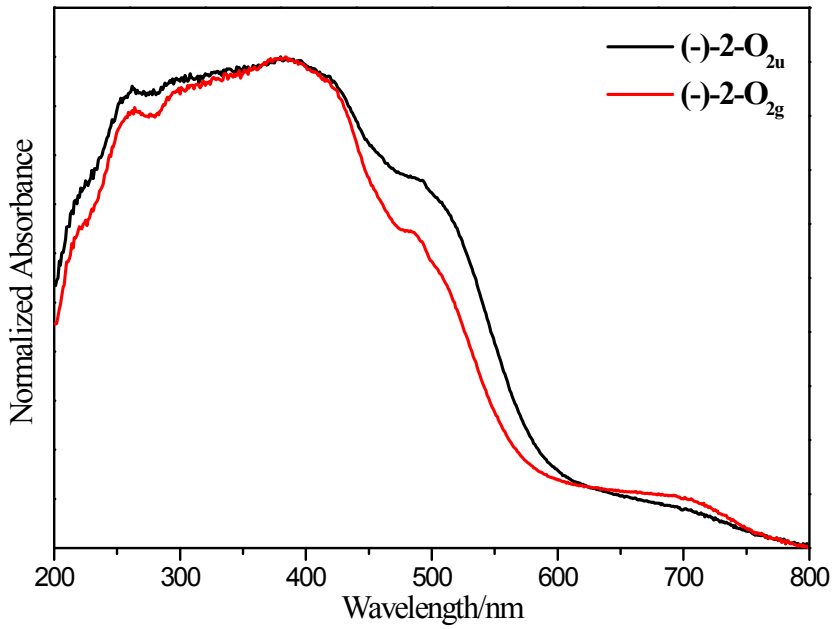

Fig. S27 Solid-state absorption spectra of (−)-**2-O$_{2u}$** in the grinding process.

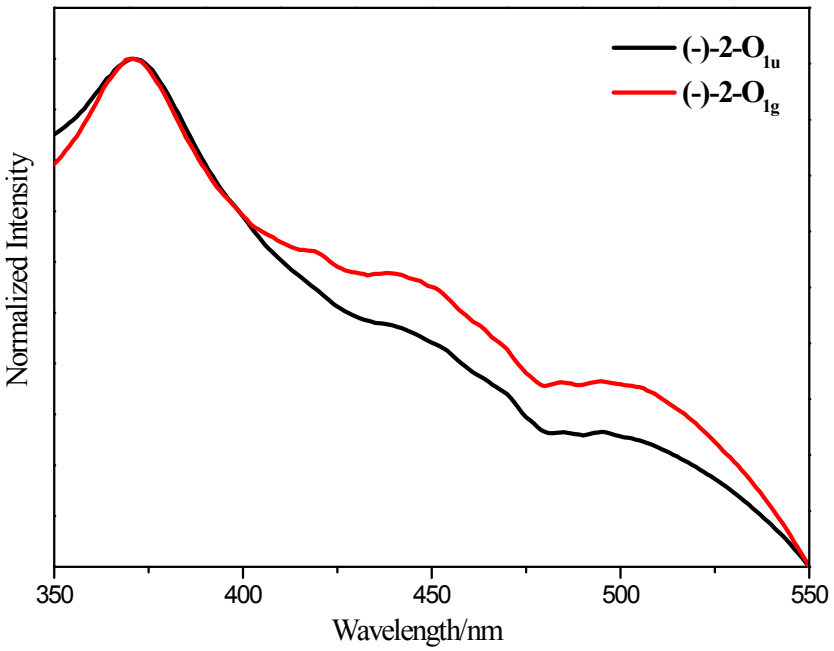

Fig. S28 Solid-state excitation spectra of (−)-**2-O$_{1u}$** in the mechanochromic process. The excitation spectra were monitored at the maximum emission peaks (λ_{em} = 626 nm nm for (−)-**2-O$_{1u}$** and (−)-**2-O$_{1g}$**).

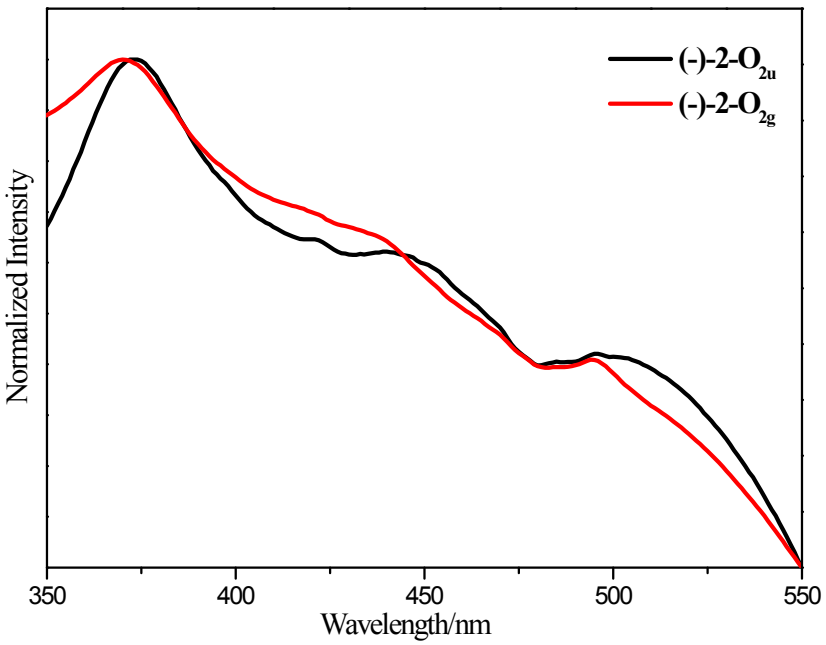

Fig. S29 Solid-state excitation spectra of (−)-**2-O$_{2u}$** in the mechanochromic process. The excitation spectra were monitored at the maximum emission peaks (λ_{em} = 626 nm nm for (−)-**2-O$_{2u}$** and (−)-**2-O$_{2g}$**).

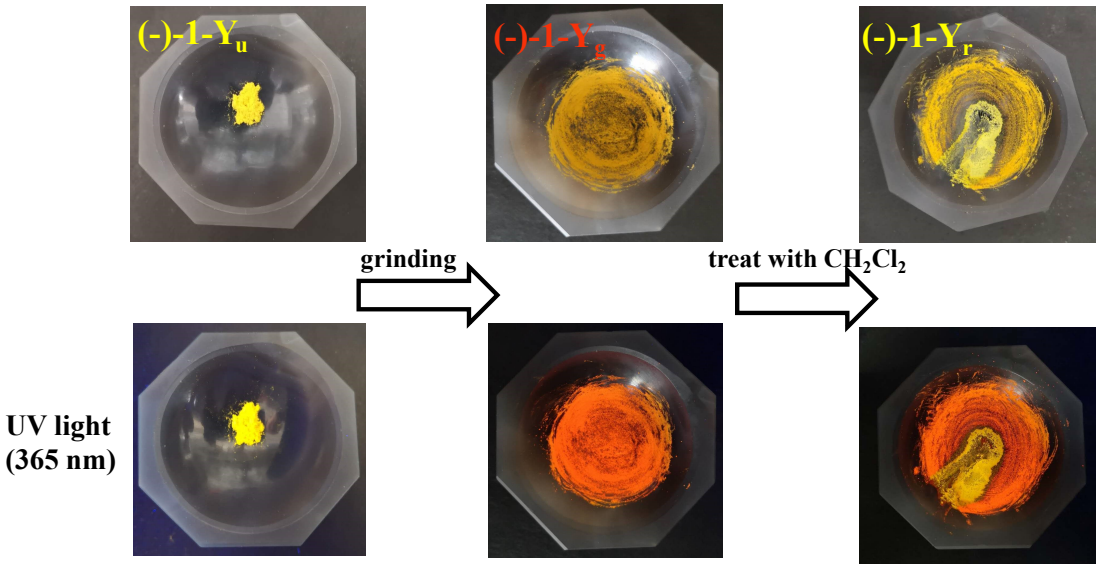

Fig. S30 Mechanochromic luminescence of (−)-**1-Y$_u$**. The images were obtained under ambient light and UV radiation (λ = 365 nm).

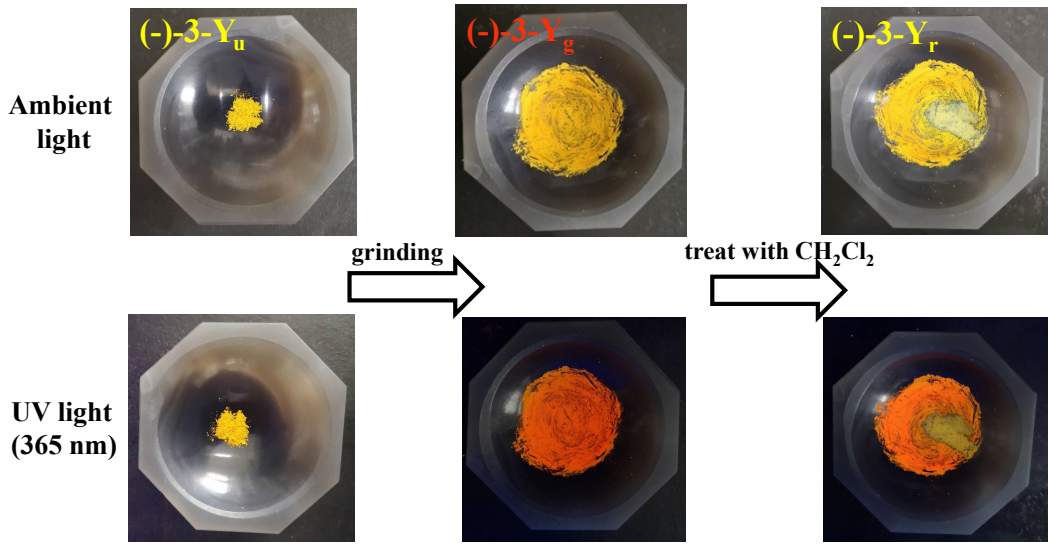

Fig. S31 Mechanochromic luminescence of (−)-**3-Y$_u$**. The images were obtained under ambient light and UV radiation (λ = 365 nm).

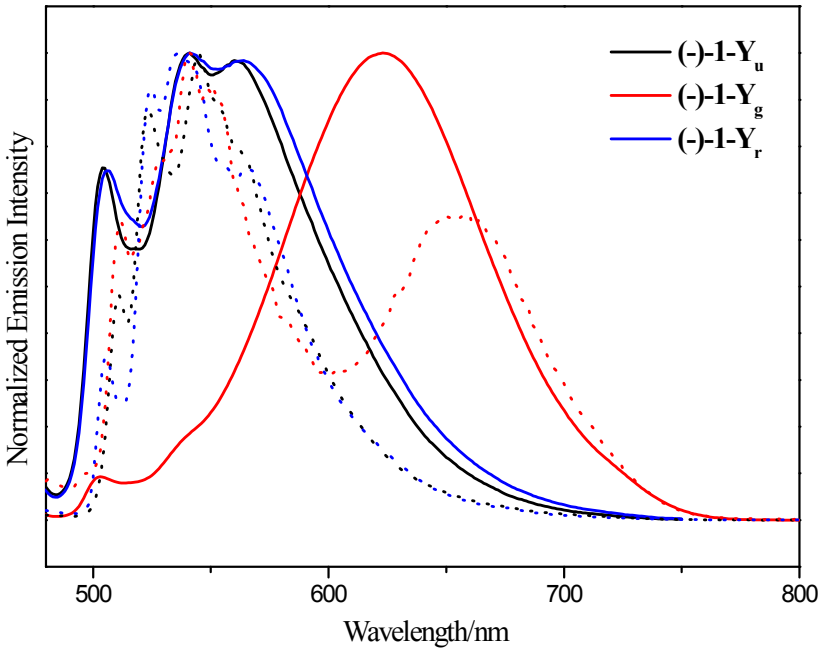

Fig. S32 Solid-state emission spectra (λ_{ex} = 420 nm) of (−)-**1-Y$_u$** in the mechanochromic process at RT (solid line) and 77 K (dot line).

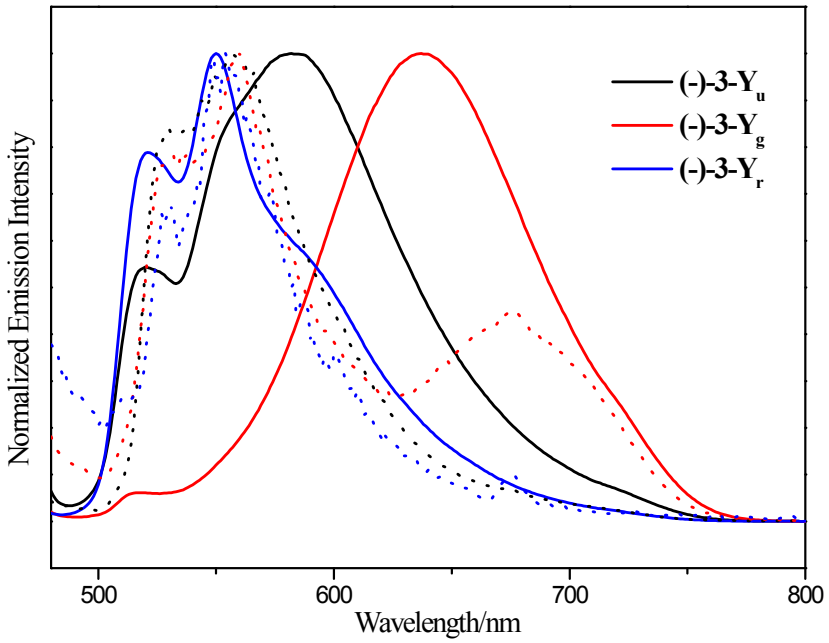

Fig. S33 Solid-state emission spectra (λ_{ex} = 420 nm) of (−)-**3-Y$_u$** in the mechanochromic process at RT (solid line) and 77 K (dot line).

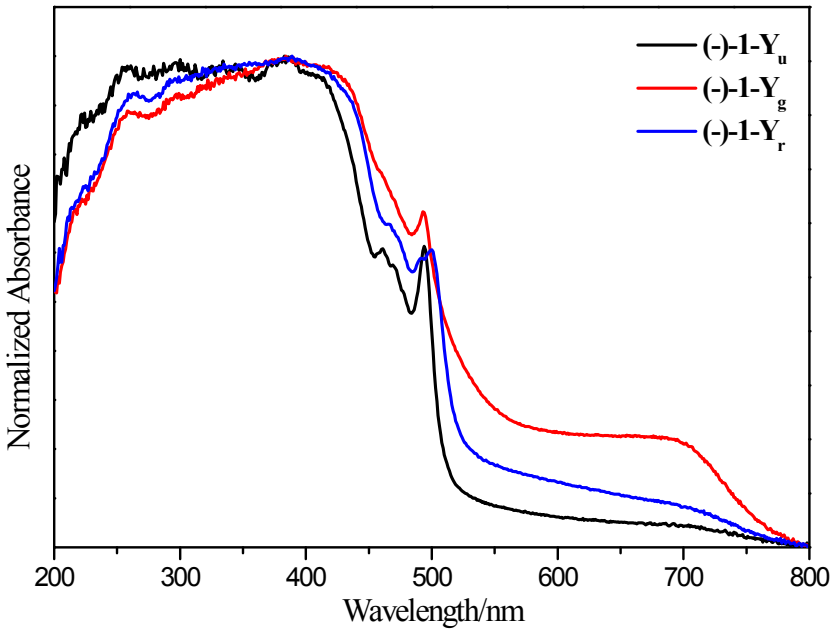

Fig. S34 Solid-state absorption spectra of (−)-**1-Y$_u$** in the mechanochromic process.

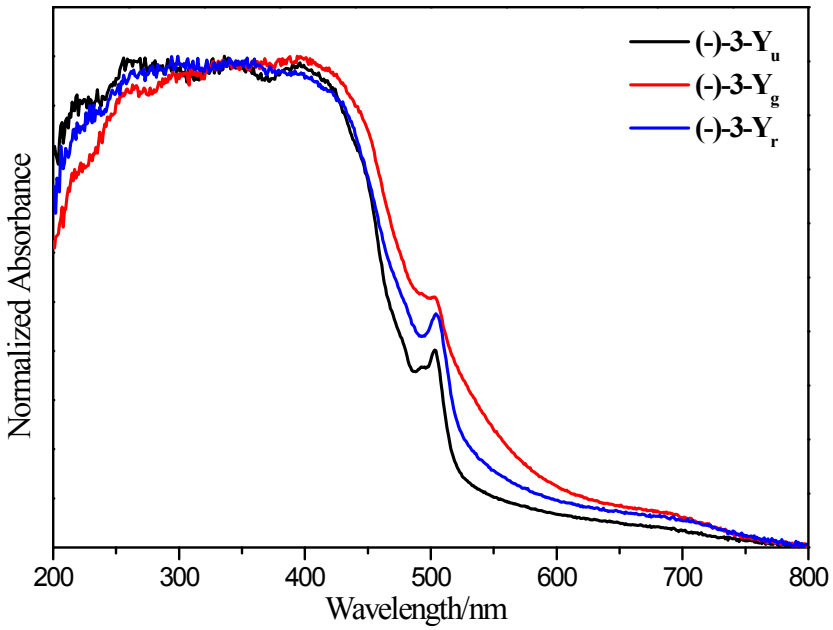

Fig. S35 Solid-state absorption spectra of (−)-**3-Y$_u$** in the mechanochromic process.

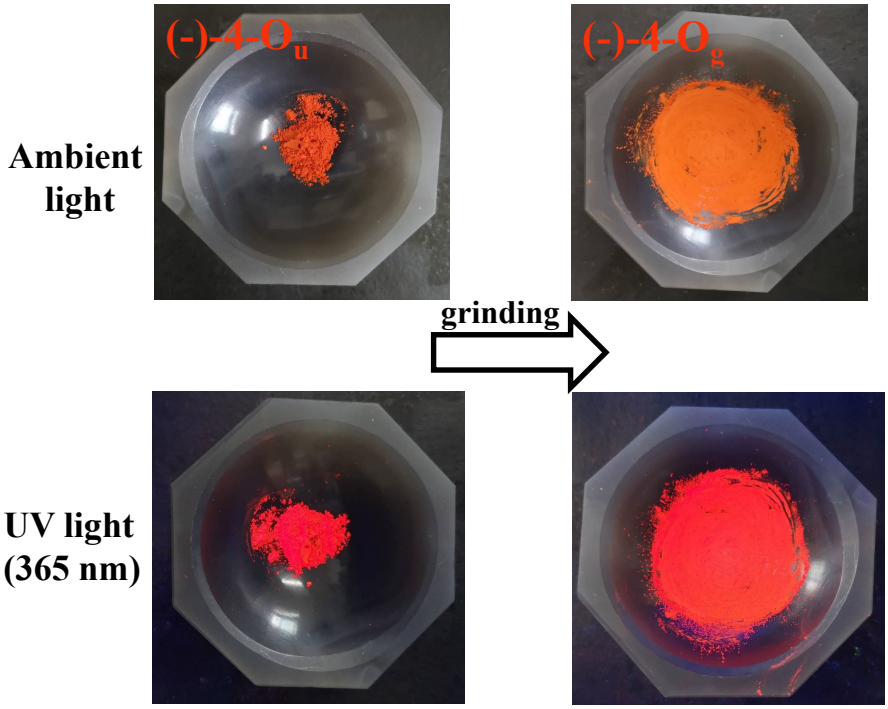

Fig. S36 Grinding process of (−)-**4-O$_u$**. The images were obtained under ambient light and UV radiation (λ = 365 nm).

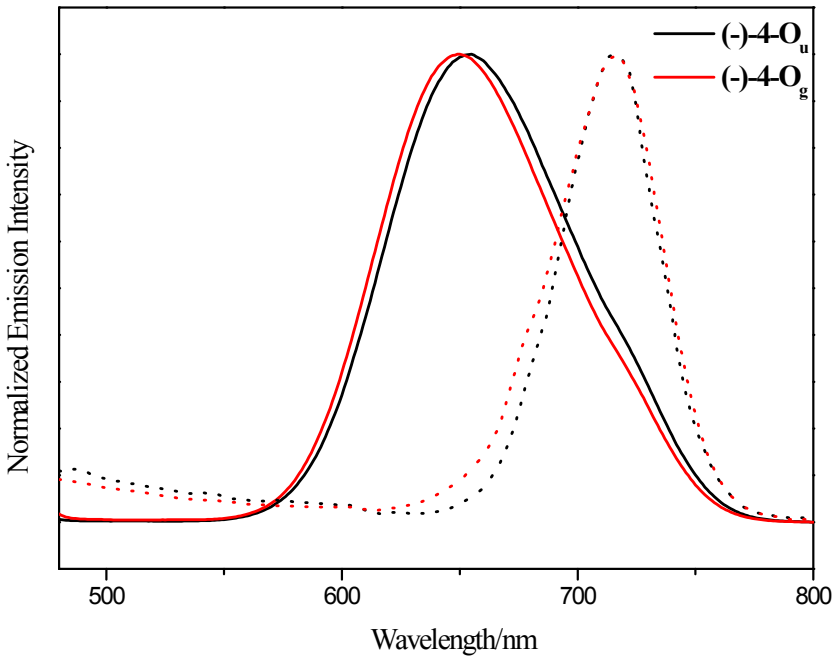

Fig. S37 Solid-state emission spectra (λ_{ex} = 420 nm) of (−)-**4-O$_u$** in the grinding process at RT (solid line) and 77 K (dot line).

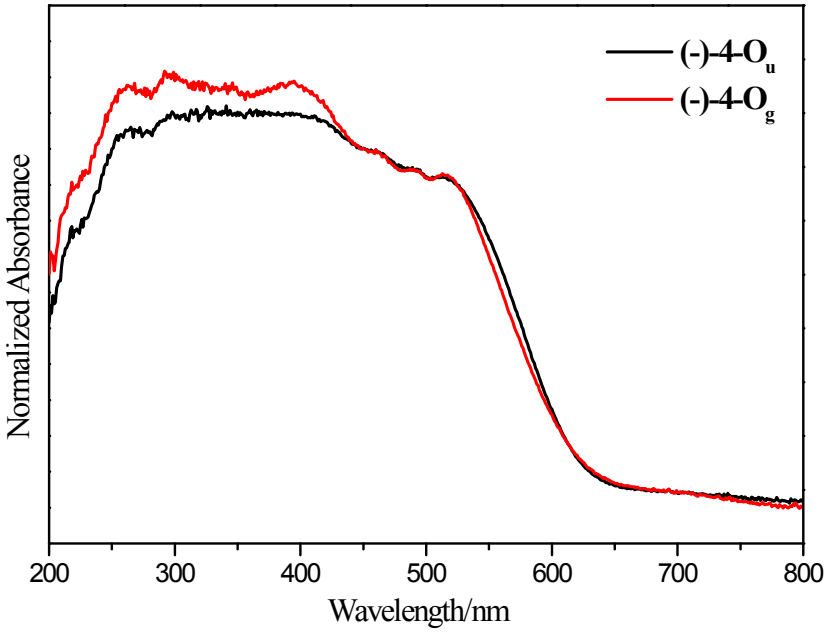

Fig. S38 Solid-state absorption spectra of (−)-**4-O$_u$** in the grinding process.

Table S6 Mechanochromic behaviors of cyclometalated Pt(NCN)Cl complexes

Complexes	Color		Emission wavelength/ nm		Emission origin	
	unground samples	ground samples	unground samples	ground samples	unground samples	ground samples
Pt(N^C^N)Cl liquid-crystalline [1]	yellow	red	575	660	$^3\pi,\pi^*$	excimer
Pt(*CH*$_3$-N^C^N)Cl [2]	yellow	orange	530	670	$^3\pi,\pi^*$	excimer
Pt(*CF*$_3$-N^C^N)Cl [3]	yellow	red	550	750	$^3\pi,\pi^*$	^{3}MMLCT
Pt(*amide*-N^C^N)Cl [4]	green	orange	512	635	$^3\pi,\pi^*$	excimer
Pt(Pa-NCN)Cl [5]	red	orange	695	681	excimer	excimer
Pt(*t*-bu-NCN)Pa [6]	yellow	red	526	675	excimer	excimer
Pt(*fluorenyl*-NCN)Cl [7]	yellow	red	521	639	$^3\pi,\pi^*$/^{3}MLCT	^{3}MLCT

6. References

[1] V. N. Kozhevnikov, B. Donnio and D. W. Bruce, *Angew. Chem. Int. Ed.,* 2008, **47,** 6286-6289;

[2] T. Abe, T. Itakura, N. Ikeda and K. Shinozaki, *Dalton Trans.,* 2009, **38,** 711-715;

[3] Y. Nishiuchi, A. Takayama, T. Suzuki and K. Shinozaki, *Eur. J. Inorg. Chem.,* 2011, **11,** 1815-1823;

[4] S. J. Choi, J. Kuwabara, Y. Nishimura, T. Arai and T. Kanbara, *Chem. Lett.,* 2012, **41,** 65-67;

[5] C.-J. Lin, Y.-H. Liu, S.-M. Peng, T. Shinmyozu and J.-S. Yang, *Inorg. Chem.,* 2017, **56,** 4978-4989;

[6] C.-Y. Lien, Y.-F. Hsu, Y.-H. Liu, S.-M. Peng, T. Shinmyozu and J.-S. Yang, *Inorg. Chem.,* 2020, **59,** 11584-11594.

[7] S.-Q Zhu, J.-Y. Hu, S.-L. Zhai, Y. Wang, Z. Xu, R. Liu and H. Zhu, *Inorg. Chem. Front.,* 2020, **7,** 4677-4686.